Chaos and incoherence in a classical rotation-vibration model of infrared multiple-photon excitation

Jay R. Ackerhalt and Peter W. Milonni
Theoretical Division T-12, Mail Stop J569, Los Alamos National Laboratory, Los Alamos, New Mexico 87545
(Received 28 September 1987)

By including rotations in a previously developed generic vibrational model of ir multiple-photon excitation (MPE) [Phys. Rev. Lett. **51**, 1259 (1983) and Phys. Rev. A **34**, 1211 (1986)] it is found that the combination of chaotic dynamics and rotational averaging leads to fluence-dependent absorption and removes the sensitivity of the results to model-dependent parameters. Therefore, a complete propagation calculation through a molecular medium of this type would show a Beer's law absorption of photons consistent with the vast majority of MPE experiments performed to date, a result which previously was attributed to rate-equation dynamics in the molecular quasicontinuum. In addition, the classical rotation-vibration dynamics observed in this model correlate very well with one's quantum intuition based on a molecule's *P*-, *Q*-, and *R*-branch structure and on the red shift of the vibrational absorption feature with excitation.

INTRODUCTION

Infrared multiple-photon excitation (MPE) of polyatomic molecules was a major area of research for roughly a decade beginning in 1971 with the work of Isenor and Richardson.[1] Their experiments showed that modest laser powers could easily dissociate a polyatomic molecule. The promise for the future was bond-selective laser photochemistry and laser isotope separation. As this research field grew over the next ten years, it became clear that molecules were not as discriminating with respect to laser wavelength and intensity as was first hoped. By the mid 1980s the field had been nearly abandoned with only a few research groups refusing to give up because a solid theoretical explanation of the phenomenon had not yet been found.

We should qualify our comments to point out that during that period from the early 1970s to the early 1980s the vast majority of experiments were performed with temporal pulse durations from 1 to 100 ns. The experiments were typically oriented toward measuring photons absorbed per molecule as a function of wavelength, incident energy or fluence, incident intensity, pressure, and temperature. The results of these experiments were based on photons in versus photons out and an estimate of the number of interacting molecules in the gas cell.[2] Eventually it was realized that self-focusing and self-defocusing were playing a major role in the interpretation of these experiments.[3] Recently, more sophisticated experiments have been undertaken using intense picosecond infrared pulses.[4,5] These experiments offer a greater understanding of how molecules absorb infrared photons and may initiate a new era of active research in this field.

As the MPE era was winding down in the early 1980s, we were aware of the data collection efforts of Judd.[6] He had graphed experimental data on roughly 50 different molecules, all on basically *the same fluence-dependent absorption curve*, after scaling out the small-signal cross section and excited population fraction. Based on this result we decided that MPE must be a general consequence of the interaction of the laser with the molecule, independent to a certain extent of an individual molecule's idiosyncrasies. Therefore we formulated a generic model of MPE incorporating only the essential features of the phenomenon.[7]

VIBRATIONAL MODEL

The Hamiltonian chosen to represent this vibrational model of MPE was

$$\hat{H}=\Delta\hat{a}^{\dagger}\hat{a}-\chi(\hat{a}^{\dagger}\hat{a})^2+\Omega(\hat{a}+\hat{a}^{\dagger}) + \sum_m(\Delta+\epsilon_m)\hat{b}_m^{\dagger}\hat{b}_m+\sum_m\beta_m(\hat{a}^{\dagger}\hat{b}+\hat{b}^{\dagger}\hat{a})\,. \quad (1)$$

where the terms in order of appearance from left to right represent the anharmonic pump mode (two terms), laser–pump-mode coupling, harmonic background modes, and the pump-mode–background-mode coupling. This form of the Hamiltonian assumes that the laser can be treated classically, the rotating-wave approximation is valid, and the excitation number is approximately conserved. The parameters describing the process are Δ, the frequency detuning of the laser from pump-mode resonance; χ, the pump-mode anharmonicity; Ω, the Rabi frequency; ϵ_m, the frequency offset of the mth background mode from the pump mode; and β_m, the coupling strength of the mth background mode with the pump mode. Several approximations were made in solving this model based on the general nature of the MPE process: the background modes are equally spaced ($\epsilon_m=\Delta_0+m\rho^{-1}$, where Δ_0 is the frequency offset of the zero mode), the background–pump-mode coupling is constant ($\beta_m=\beta$), and since it takes roughly 30 to 40 photons to dissociate many of the larger molecules such as SF_6, the dynamics can be solved classically. In addition, the parameters were chosen to be consistent with one's knowledge of molecules: Δ specified for *Q*-branch

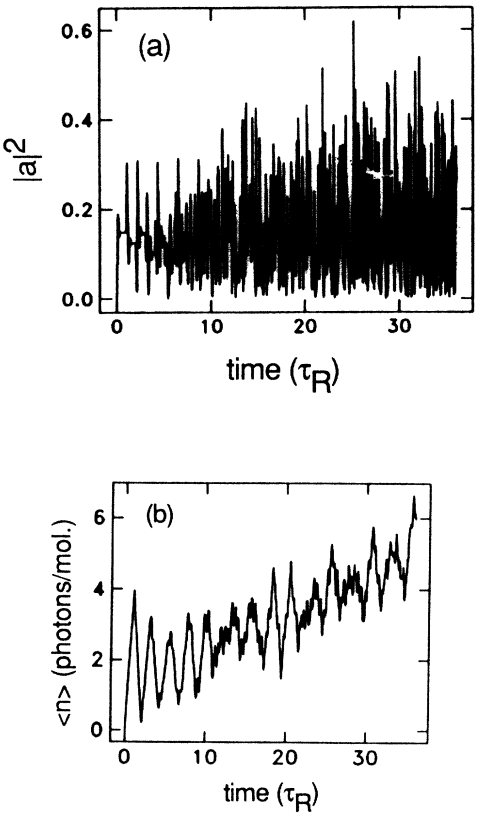

FIG. 1. (a) Number of quanta in the pump mode vs time (τ_R); (b) total quanta in the molecule vs time (τ_R). Parameters given in the text.

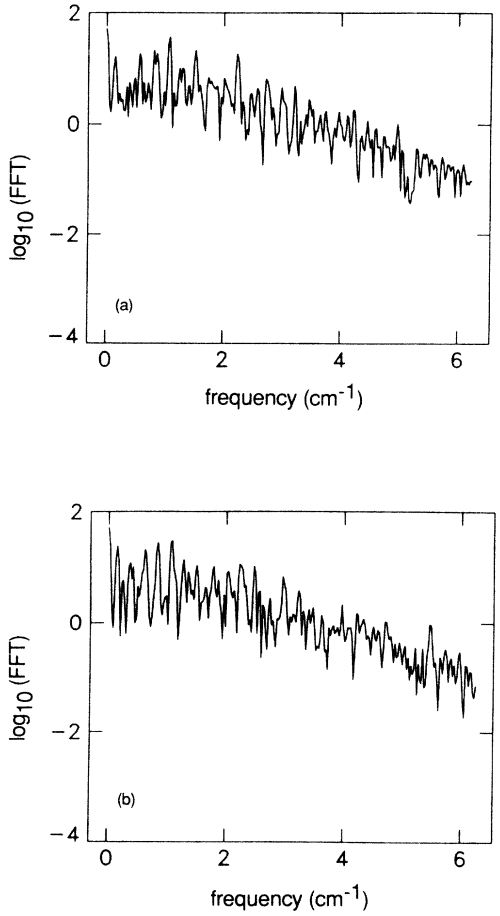

FIG. 2. Logarithmic plot of FFT vs frequency (cm^{-1}): (a) $a(0)=0$; (b) $a(0)=(0.05\sqrt{2})e^{i\pi/4}$.

excitation, $\chi=2$ cm^{-1}, $\Omega=0.3$ cm^{-1} consistent with roughly 10 MW/cm^2 in SF_6, $\rho=4/cm^{-1}$, and $\beta=0.2$ cm^{-1}.

Using the Hamiltonian (1), making the approximation that the number of background modes is infinite (an approximation justified in the context of radiationless transition theory by Bixon and Jortner[8,9]), eliminating the background modes, and simplifying the equations using the Poisson summation formula,[10] the dynamical equations of motion become

$$\dot{a}(t)=-i(\Delta-\chi)a(t)+2i\chi\,|\,a(t)\,|^2a(t) \\ -i\Omega-(\gamma/2)a(t)-\gamma s(t)\,, \tag{2a}$$

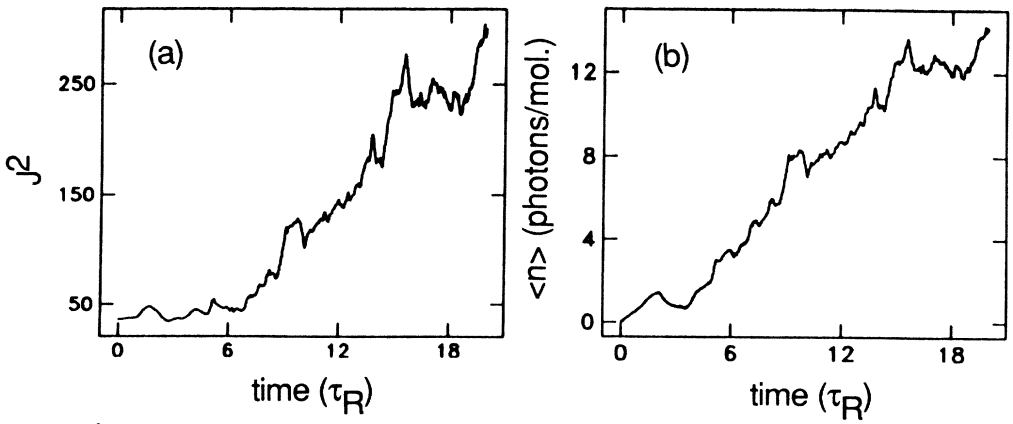

FIG. 3. (a) J^2 vs time (τ_R); (b) total quanta in the molecule vs time (τ_R), Q-branch excitation ($\Delta=2.0$ cm^{-1}).

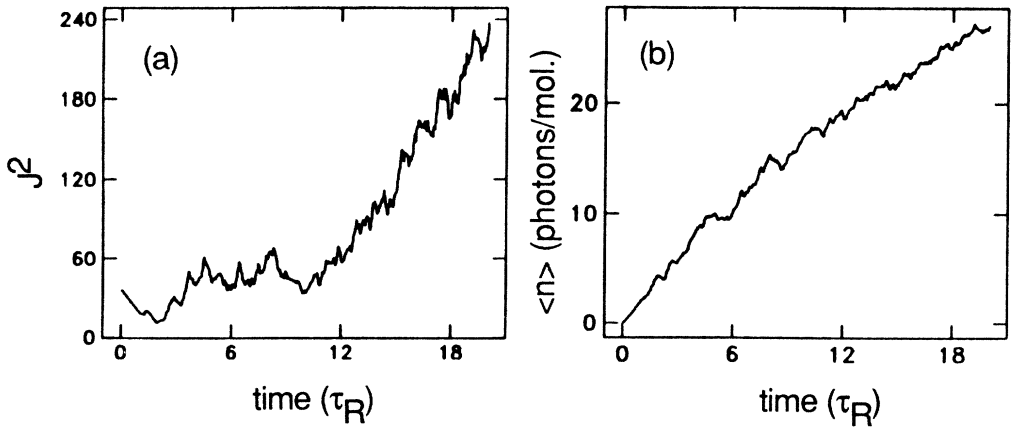

FIG. 4. Same as Fig. 3, but with P-branch excitation ($\Delta=3.2\ \mathrm{cm}^{-1}$).

$$s(t)=e^{-i\phi}[s(t-\tau_R)+a(t-\tau_R)]\ , \tag{2b}$$

where $\gamma\equiv 2\pi\beta^2\rho$ is the Fermi golden rule rate, $\tau_R\equiv 2\pi\rho$ is the memory recurrence time caused by having an equally spaced background, and $\phi\equiv(\Delta+\Delta_0)\tau_R$. In Figs. 1(a) and 1(b) we show the results of integrating Eqs. (2) with $a(0)=0$ and $\phi=\pi/2$ for $|a(t)|^2$ and the total photons absorbed versus time, respectively. The total absorbed photons have some initial regularity, but after roughly $8\tau_R$ begin an average linear growth whose slope is dependent on the initial choice of ϕ. In previous calculations for similar parameter regimes the observed dynamics were shown to be chaotic by computing the maximal Lyapunov exponent. In Fig. 2(a) we show a fast Fourier transform (FFT) of the dynamics shown in Fig. 1(a) (note the characteristic broadband spectrum of chaos). In Fig. 2(b) we show another FFT of the same dynamics as shown in Fig. 1(a), except the initial condition has been slightly modified $a(0)=(0.05\sqrt{2})e^{i\pi/4}$. The spectra shown in Figs. 2 are very different considering the rather small change in initial condition. This high degree of spectral sensitivity to initial conditions is a nonrigorous but inexpensive measure of chaotic dynamics, as FFT computations are much faster than the corresponding Lyapunov-exponent calculations. Since the laser pulse envelope is square, the linear absorption of photons reflects a fluence-dependent absorption, consistent with experimental trends. In fact, we have argued that the chaotic absorption of photons is the bond that links the fluence dependence shown by so many different molecules. However, the sensitivity of the slope to ϕ is an unsettling feature of this model.

It is interesting to point out that chaotic dynamics and an average linear energy growth in time have been observed in other systems. Casati *et al.* found this same type of energy growth in the periodically kicked pendulum.[11] Similar results were reported by Leopold and Percival, who considered a classical model of a hydrogen atom in a sinusoidal electric field.[12] Further related work was recently described by van Leeuwan *et al.*, who report excellent agreement between their classical computations and their experiments on the microwave ionization

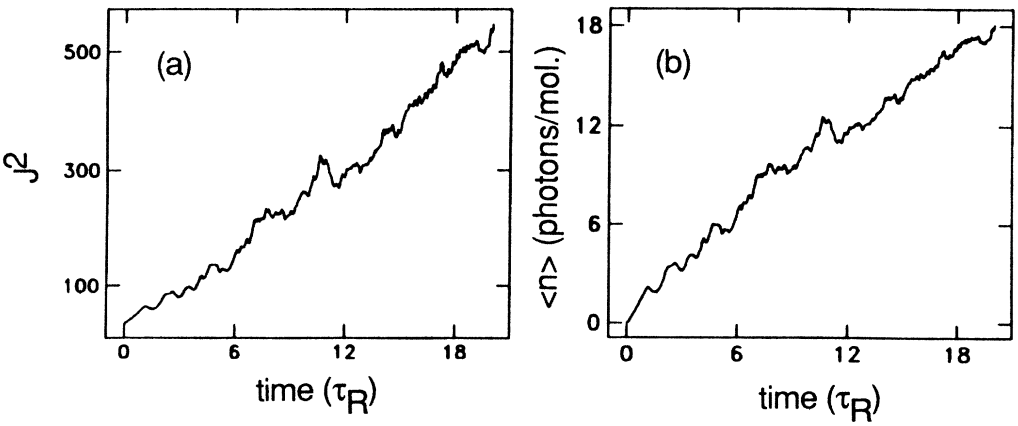

FIG. 5. Same as Fig. 3, but with R-branch excitation ($\Delta=0.8\ \mathrm{cm}^{-1}$).

of hydrogen.[13] This research coupled with our own work on MPE illustrates the importance of chaos in these driven systems.

In order to make a real comparison with experiment it is necessary to couple Maxwell's equations with the equations governing the molecular medium. We have performed these calculations, but as in the model presented above, a strong sensitivity to ϕ was found.[14] Therefore, any treatment of MPE which had any hope of comparing directly with experiment must include a molecule's rotational structure.

ROTATIONAL MODEL

Including rotations at lowest order in a classical MPE model was previously done by Galbraith *et al.*[15] In this case the pump mode was harmonic, and no background modes were included in the model. The resulting chaotic dynamics occurred entirely from the (nonlinear) coupling of the rotation of the molecule with respect to the linearly polarized electric field of the laser. The rotational dynamics were contained in the dipole coupling term which consisted of the laser in the laboratory frame and the vibrational dipole moment in the molecular frame. In related work Jones and Percival found that even for constant rotational angular momentum the additional time dependence in the dipole coupling term was sufficient to give a fluence-dependent absorption, which was not exhibited by their purely vibrational model.[16]

Following the work of Galbraith *et al.*, we have included rotations in this quasicontinuum model of MPE. The Hamiltonian (1) becomes

$$\hat{H}=\Delta\hat{a}^{\dagger}\hat{a}-\chi(\hat{a}^{\dagger}\hat{a})^2+\Omega P_3(\hat{a}+\hat{a}^{\dagger})+\sum_m(\Delta+\epsilon_m)\hat{b}_m^{\dagger}\hat{b}_m+\sum_m\beta_m(\hat{a}^{\dagger}\hat{b}+\hat{b}^{\dagger}\hat{a})+B_0(\hat{J}_1^2+\hat{J}_2^2)\,, \tag{3}$$

where the laser-molecule coupling term has been modified to include the direction cosine matrix of the molecule relative to the linearly polarized electric field of the laser, oriented along the 3-axis in the laboratory frame. The last term represents the rotation of the molecule about the 1- and 2-axes. This model is simplified in that the nondegenerate pump mode, oriented along the 3-axis in the molecular frame, is treated as a diatomic molecule, so that it has no rotational angular momentum along that direction. This simplification of the molecular model is purely for convenience, since we believe that the complexity of having a full triply degenerate pump mode with three rotational degrees of freedom is a detail offering no additional physical insights into the chaotic dynamics of rotating molecules. Obviously a model of a molecule like SF_6 would require this additional calculational complexity. The value of B_0 is chosen as 0.1 cm^{-1} in all cases.

The dynamical equations governing this system, making all the same assumptions as was done for Eqs. (2), are

$$\dot{a}(t)=-i(\Delta-\chi)a(t)+2i\chi\,|a(t)|^2a(t)-i\Omega P_3(t)-(\gamma/2)a(t)-\gamma s(t)\,, \tag{4a}$$

$$s(t)=e^{-i\phi}[s(t-\tau_R)+a(t-\tau_R)]\,, \tag{4b}$$

$$\dot{J}_1(t)=\Omega P_2(t)[a(t)+a^{\dagger}(t)]\,, \tag{4c}$$

$$\dot{J}_2(t)=-\Omega P_1(t)[(a)+a^{\dagger}(t)]\,, \tag{4d}$$

$$\dot{P}_1(t)=-2B_0J_2(t)P_3(t)\,, \tag{4e}$$

$$\dot{P}_2(t)=2B_0J_1(t)P_3(t)\,, \tag{4f}$$

$$\dot{P}_3(t)=-2B_0[J_1(t)P_2(t)-J_2(t)P_1(t)]\,, \tag{4g}$$

where for ease in comparing results from this model with the earlier vibrational model, we have specified $P_3(0)=1$, $P_2(0)=P_1(0)=J_2(0)=0$. Therefore, we recover the previous vibrational model for $J_1(0)=0$ and have a simple rotational model for $J_1(0)\neq 0$. A description of the derivation of these equations is given in Ref. 15. From Eqs. (4) the absorbed rotational and vibrational quanta in the molecule are

$$J_1^2(t)+J_2^2(t)=-2\frac{\Omega}{B_0}\int_0^t\dot{P}_3(t')\mathrm{Re}[a(t')]dt'\,, \tag{5a}$$

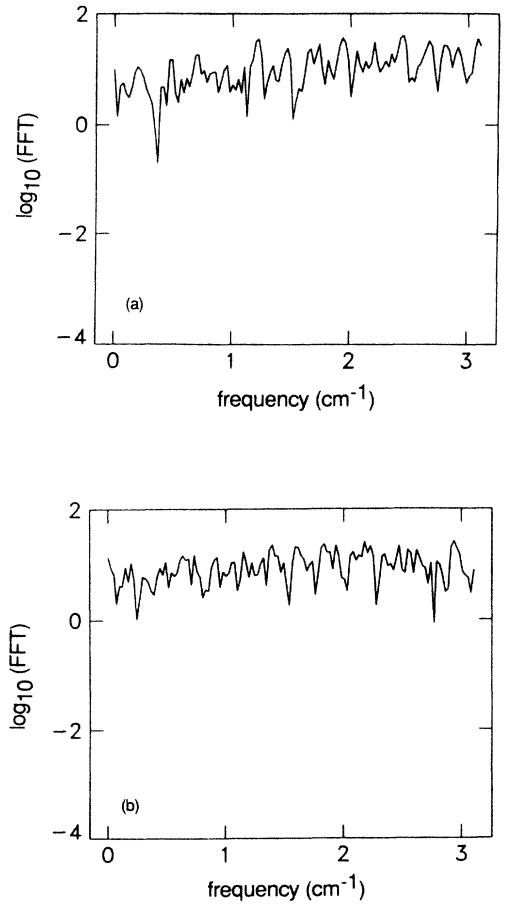

FIG. 6. Logarithmic plot of FFT vs frequency (cm^{-1}) for parameters of Fig. 3, but with $\phi=0$, (a) $a(0)=0$, (b) $a(0)=(0.015\sqrt{2})e^{i\pi/4}$.

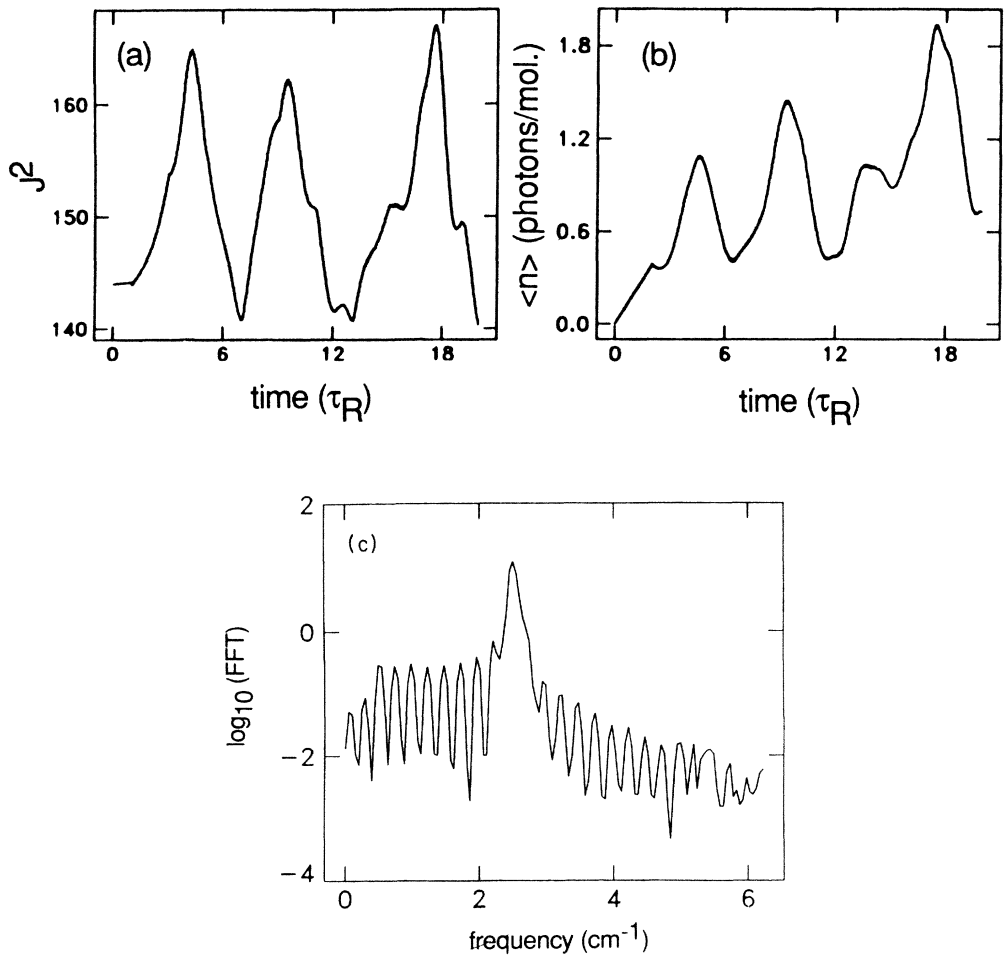

FIG. 7. (a) J^2 vs time (τ_R); (b) total quanta in the molecule vs time (τ_R); (c) logarithmic plot of FFT vs frequency (cm^{-1}) for Q-branch excitation ($\Delta=2.0\ cm^{-1}$) and $J_1(0)=12$.

$$a^{\dagger}(t)a(t)+\sum_m b_m^{\dagger}(t)b_m(t) = -2\Omega\int_0^t P_3(t')\mathrm{Im}[a(t')]dt' . \quad (5b)$$

In Figs. 3(a) and 3(b) we show the square of the rotational angular momentum and photons absorbed per molecule versus time, respectively, computed using Eqs. (4) and (5) with $J_1(0)=6$. All other parameters have been chosen the same as in Figs. 1. Two aspects of these figures should be noted: the regular region shown in Fig. 1(b) in the early-absorption regime is absent in Fig. 3(b), and the rotational absorption to some extent closely parallels the vibrational absorption. In Figs. 4 and 5 we show the exact same dynamics as in Figs. 3, but for the P and R branches, respectively, i.e., $\Delta=3.2\ cm^{-1}$ and $\Delta=0.8\ cm^{-1}$. In comparing Figs. 3–5, one immediately notices that the overall absorption is sensitive to detuning. In addition, the R-branch rotational absorption curve very closely parallels the corresponding vibrational absorption curve in both shape and number of quantum changes. This is not completely surprising, since in the R branch $\Delta J=1$, consistent with a one-to-one correspondence between vibrational and rotational absorption of quanta. What is perhaps surprising is that this calculation is completely classical.

In Figs. 3 and 4 one notices that the P branch ($\Delta J=-1$) curve for J^2 shows an initial decrease, a flat region, and an increasing region. This is again entirely consistent with our quantum intuition, since the anharmonicity of the pump mode shifts the absorption feature to the red with increasing vibrational excitation making the rotational dynamics shift from P- to Q- to R-branch absorption. Our quantum intuition also works well in describing the Q-branch results shown in Fig. 3. In all cases studied, the correspondence between rotational and vibrational quantum changes was in very good agreement with our expectations from quantum mechanics in both magnitude and direction.

In Fig. 6(a) we show an FFT spectrum for the parameters of Fig. 3, but with $\phi=0$. Note the broadband irregular spectrum characteristic of chaos. In Fig. 6(b) we show a corresponding spectrum where the initial conditions have been slightly modified $a(0)=(0.015\sqrt{2})e^{-\pi/4}$. Comparing Figs. 6(a) and 6(b) shows an extreme sensitivi-

ty to initial conditions indicating that the dynamics remain chaotic when the vibrational model (1) is allowed to rotate. These results for the FFT spectrum are typical of all the rotational calculations performed.

If the rotational angular momentum is initially increased to a value much greater than $J_1(0)=6$, then we may expect to find some degree of rotational stabilization of the molecule, as was found in Ref. 15. In Figs. 7(a)–7(c) we show the square of the rotational angular momentum versus time, the photons absorbed per molecule versus time, and an FFT spectrum of the time dynamics of $a(t)$ versus frequency, respectively, for the same parameter values as those of Fig. 3, except $J_1(0)=12$. Compared to Fig. 3 the number of photons absorbed and the change in the rotational angular momentum are very small. The overall absorption is not even large enough for the absorption feature to have red shifted from the Q branch into the R branch. The dynamics also do not show the diffusive growth in energy seen previously. In fig. 7(c) the spectrum shows a dominant feature at $2B_0J=2.4$ cm^{-1} and no significant feature at the Q branch or zero frequency explaining the lack of excitation. In this instance $J_1(0)$ is obviously large enough to give the molecule a gyroscopic stabilization, as observed in Ref. 15. In Figs. 8(a)–8(c) we show the result of changing the laser frequency to the P branch $\Delta=4.4$ cm^{-1}. In this case we see a return to strong diffusive energy growth and chaos. The FFT spectrum no longer shows a distinct absorption feature at $2B_0J_1(0)$ and is reminiscent of a broadband chaotic spectrum. Note also the characteristic transition in J^2 from P- to Q- to R-branch dynamics in Fig. 8(a) as the absorption feature is red shifted. In Figs. 9(a)–9(c) we show the R-branch dynamics $\Delta=-0.4$ cm^{-1}, in the same format as in Figs. 7 and 8. Again we observe absorption dynamics showing a diffusive energy growth and a broadband FFT spectrum, both representative of chaos. It would appear that for high initial rotational angular momentum only a window about the Q branch is gyroscopically stabilized. The P and R branches are dynamically similar and described by a chaotic absorption of photons. While this chaotic dynamics is consistent with experiment, the slope

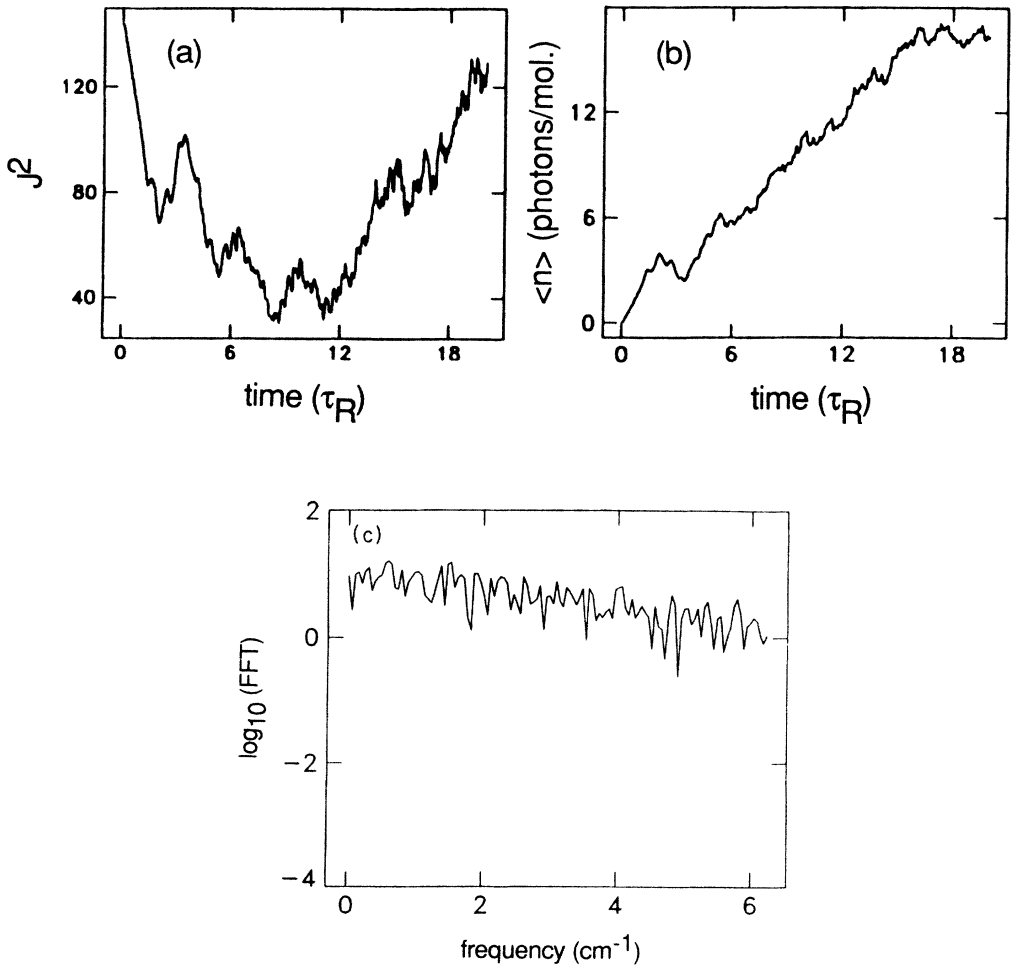

FIG. 8. Same as Fig. 7, except for P-branch excitation ($\Delta=4.4$ cm^{-1}).

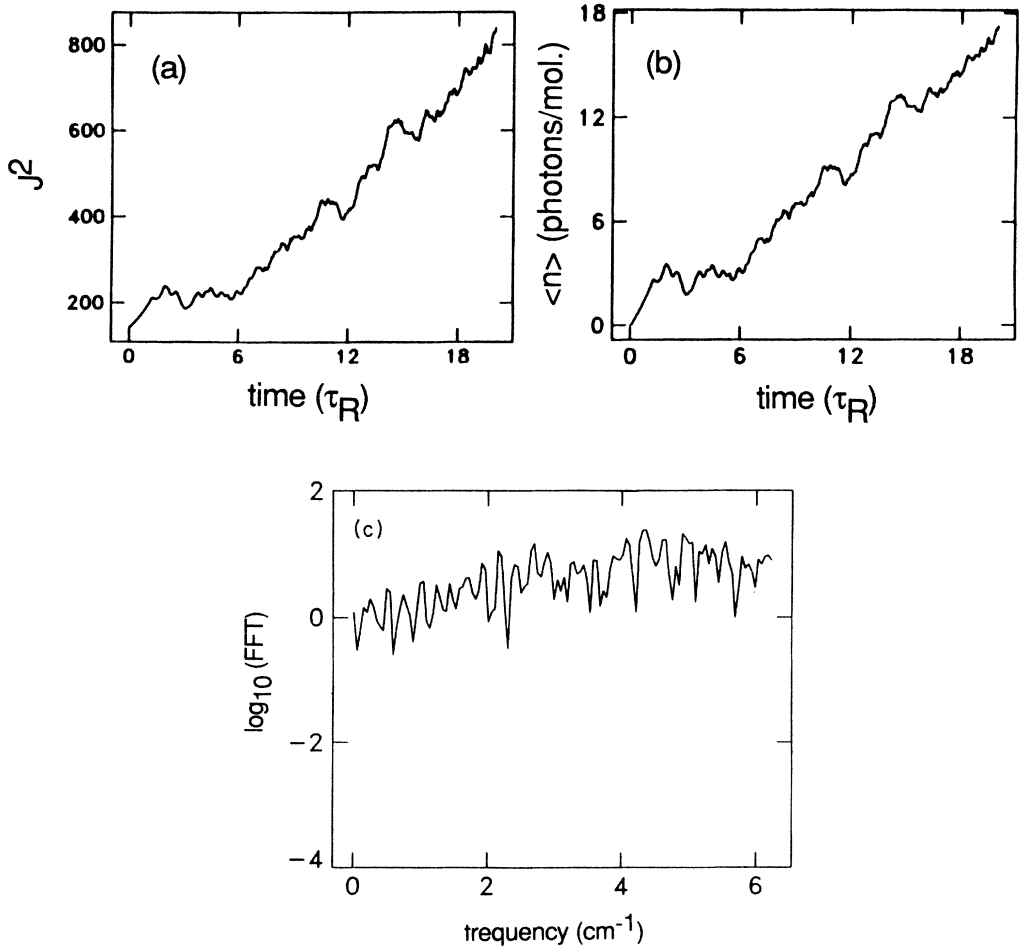

FIG. 9. Same as Fig. 7, except for R-branch excitation ($\Delta = -0.4\ cm^{-1}$).

observed in Figs. 7–9 is very sensitive to the specific choice of ϕ. In Figs. 10(a) and 10(b) we show analogous results to Figs. 8(a) and 8(b), but with $\phi = 0$. Notice the distinct differences in the dynamics. Since we are looking for a generic description of MPE, this is a very disturbing feature of the model. A remedy for this problem will be given in the following section.

Since the chaotic absorption of photons for cases where $J_1(0) > 0$ and the pulse envelope is square showed linear absorption over the entire time interval with no initial regular period as in Fig. 1, it is important to verify the fluence dependence of the absorption process by

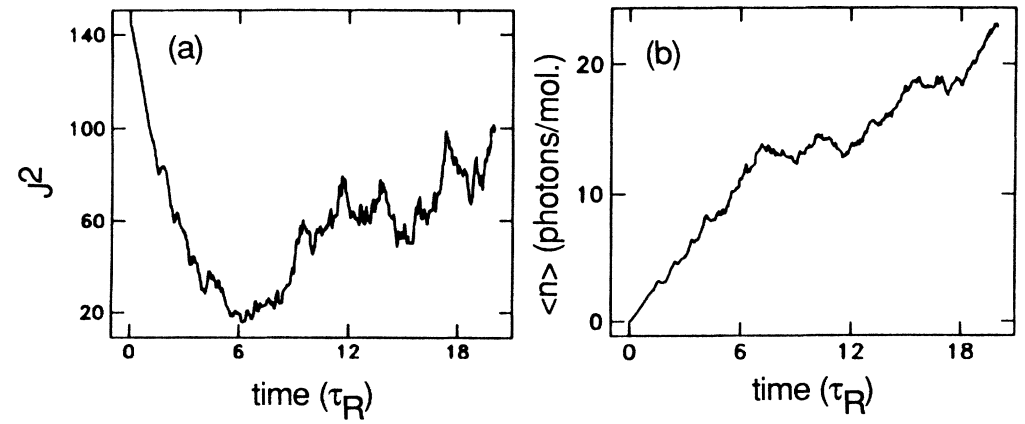

FIG. 10. Same as Figs. 8(a) and 8(b), but with $\phi = 0$.

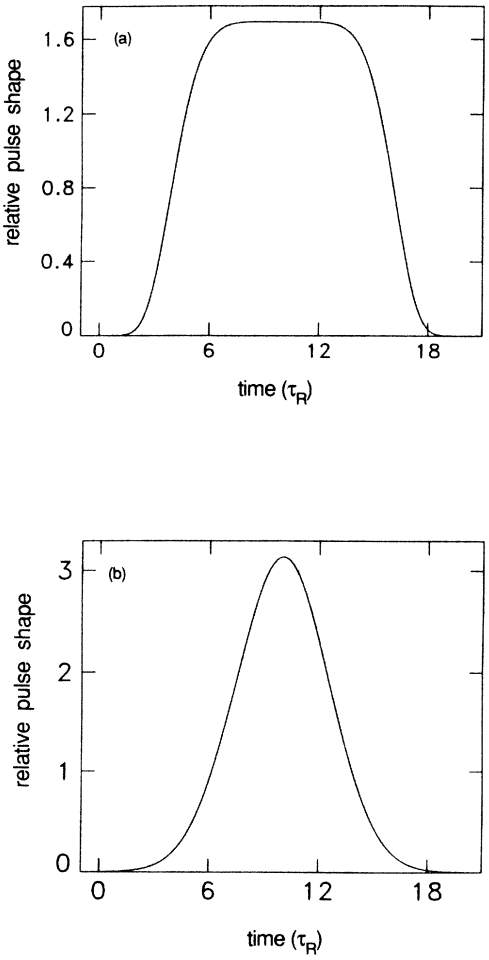

FIG. 11. Electric field pulse shapes vs time (τ_R), (a) broad high-order super-Gaussian; (b) narrow Gaussian

studying cases where the electric field envelope is time dependent. Two pulse formats have been studied: one a fairly wide super-Gaussian and the other a moderately narrow Gaussian, both shown in Figs. 11(a) and 11(b), respectively. The two pulses were chosen to have the same fluence. In Figs. 12 and 13 we show the excitation using the same parameters of Fig. 3, but with the excitation due to pulse envelope formats represented by Figs. 6(a) and 6(b), respectively. A comparison of these figures shows the very strong fluence (rather than intensity) dependence of the absorption.

MOLECULAR MODEL

The rotational model of a molecule just discussed only represents the absorption of one temperature group of molecules in a Boltzmann distribution. Therefore, we have performed calculations averaging over a complete Boltzmann distribution in order to obtain a realistic description of the overall molecular dynamics. Even though these calculations are classical we have used a quantum description for the density of states, as we believe the specific choice of distribution function is of no consequence here:

$$P(J)=(B_0/kT)(2J+1)e^{-B_0J(J+1)/kT}, \tag{6}$$

where the Boltzmann constant k is equal to 0.72 in units where B_0 is in cm^{-1} and T is in degrees kelvin. The peak of the distribution is given by

$$J_{\mathrm{peak}}=(0.36T/B_0)^{1/2}-\tfrac{1}{2} \tag{7}$$

and the integrated probability by

$$I=\int_{J_1}^{J_2}P(J)dJ = e^{-B_0J_1(J_1+1)/kT}-e^{-B_0J_2(J_2+1)/kT}. \tag{8}$$

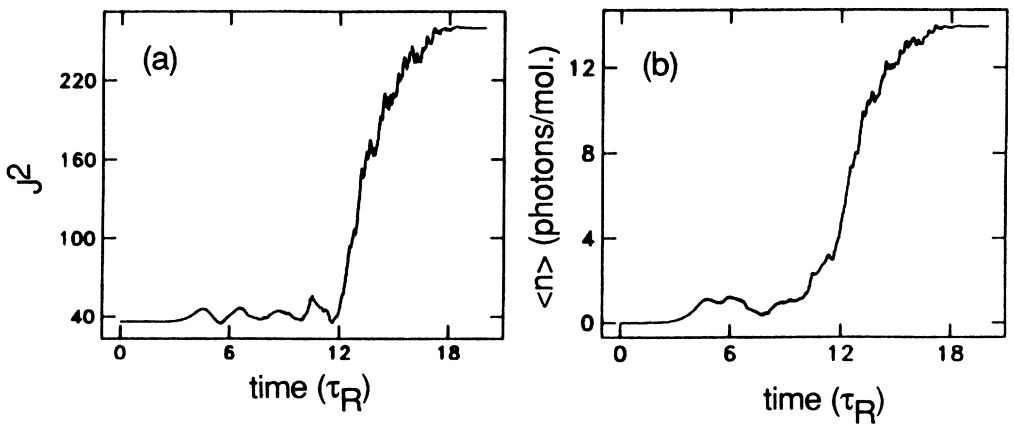

FIG. 12. Same as Fig. 3, but with pulse shape shown in Fig. 11(a).

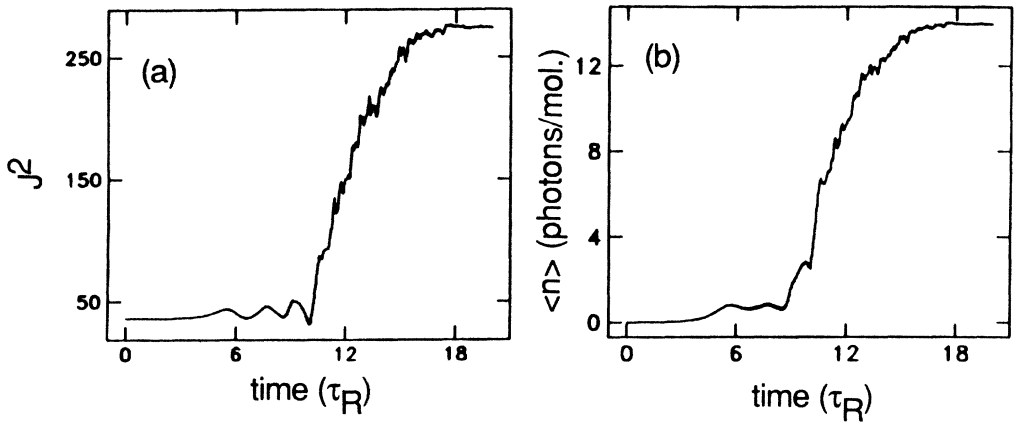

FIG. 13. Same as Fig. 3, but with pulse shape shown in Fig. 11(b).

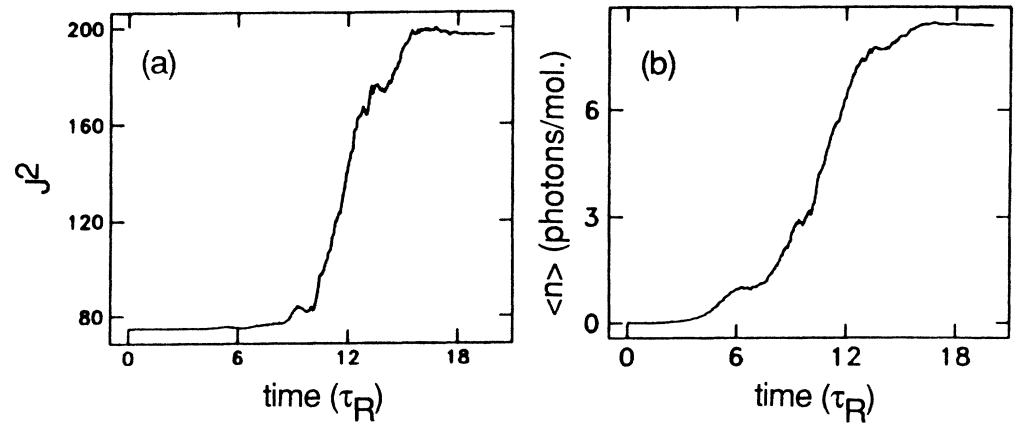

FIG. 14. Same parameters and pulse format as in Fig. 13, but Boltzmann averaged at a temperature of 11.74 K. Peak J equals 6 with 99% of the population contained in region $0 \leq J \leq 20$.

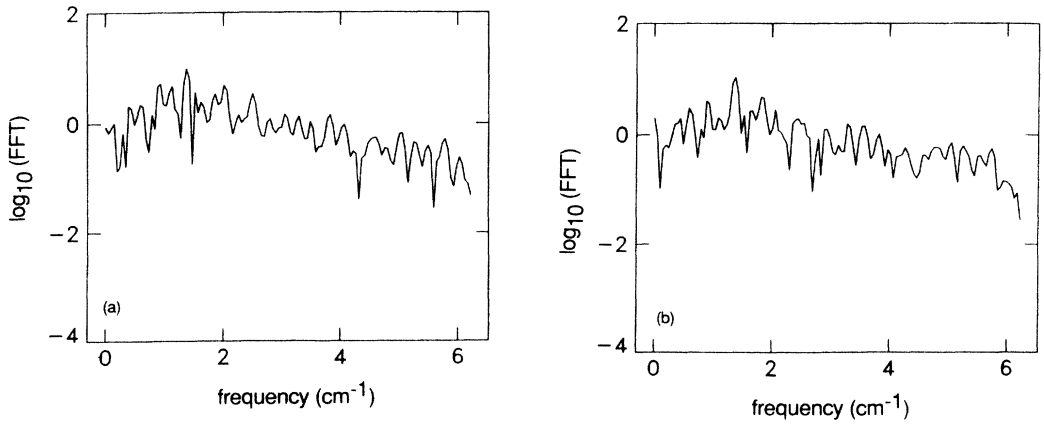

FIG. 15. Logarithmic plot of FFT vs frequency (cm^{-1}) for parameters of Fig. 14; (a) $a(0)=0$, (b) $a(0)=(0.007\sqrt{2})e^{i\pi/4}$.

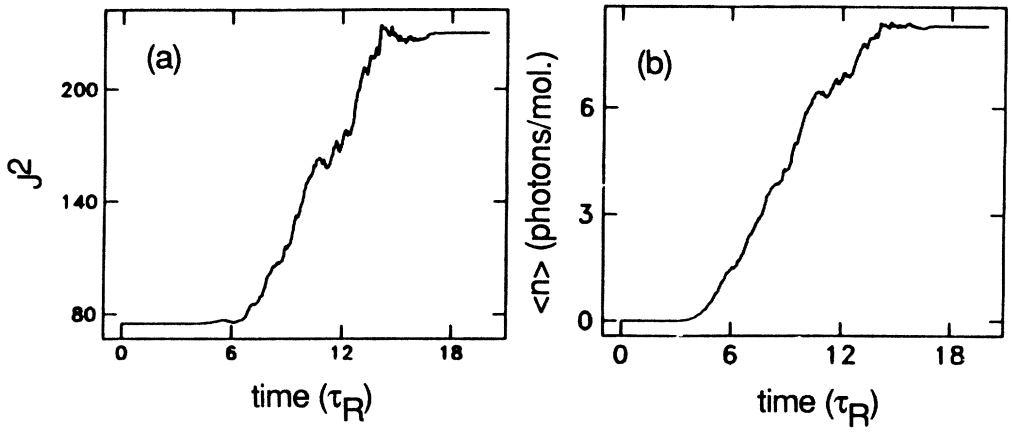

FIG. 16. Same as Fig. 14, but using pulse format of Fig. 11(a).

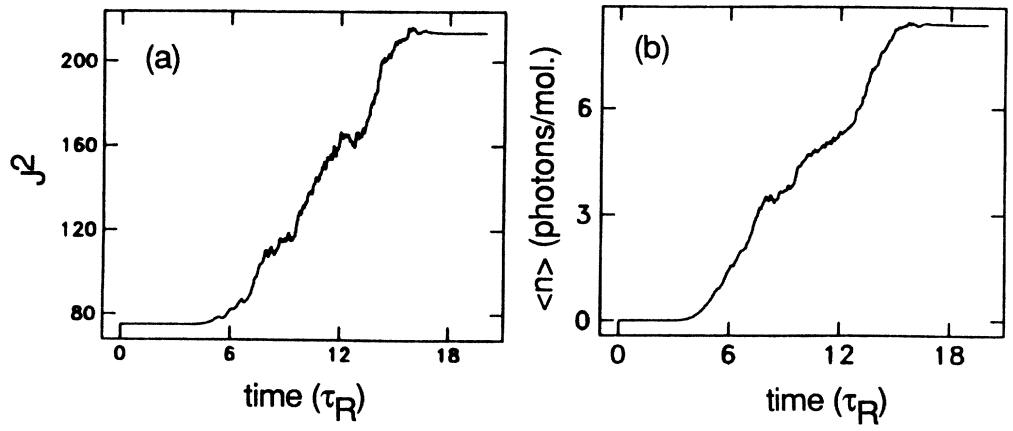

FIG. 17. Same as Fig. 16, except $\phi=0$.

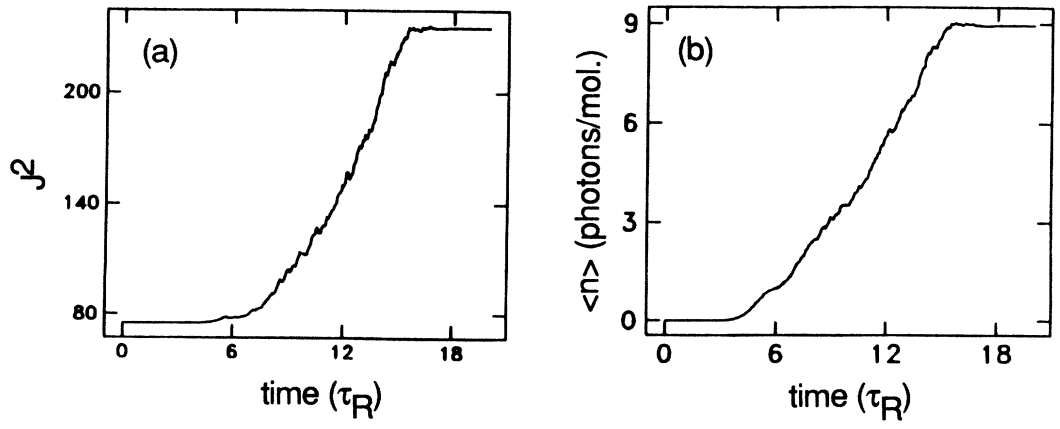

FIG. 18. Same as Fig. 16, except $\phi=\pi$.

For simplicity the results are presented for a temperature of 11.74 K which gives a distribution peaked at $J=6$ and an integrated probability distribution from $J_1=0$ to $J_2=20$ of greater than 99%. Eleven different initial J values from 0 to 20 counting by twos are averaged and weighted by the appropriate Boltzmann factor computed using (6). In Figs. 14(a) and 14(b) we show the results of a Boltzmann-averaged calculation for Q-branch excitation using the parameters and pulse format of Fig. 13. The excitation is reduced from Fig. 13 because of the off-resonant contributions to the excitation. The dynamics look chaotic but are substantially smoothed out by the averaging. In Fig. 15(a) a FFT of the time dynamics of $a(t)$ shows a broadband spectrum indicating chaos. In Fig. 15(b) the initial condition for $a(t)$ has been slightly shifted $a(0)=(0.007\sqrt{2})e^{i\pi/4}$. A comparison of Figs. 15(a) and 15(b) strongly suggests that the full Boltzmann-averaged dynamics are chaotic. In Figs. 16(a) and 16(b) the results of the same calculation are shown, except that the pulse format has been changed to that shown in Fig. 11(a). Comparing Figs. 14 and 16 confirms the fluence dependence of these averaged calculations. In Figs. 17(a) and 17(b) [(18(a) and 18(b)] we show the results of changing ϕ from $\pi/2$ to 0 (π). Comparing Figs. 16, 17, and 18 shows that these *averaged calculations are no longer ϕ dependent* making the general nature of this model complete. We have also studied P-branch and R-branch dynamics confirming this very exciting result.

CONCLUSIONS

Overall the Boltzmann rotationally averaged calculations show only minimal dependence on the molecular model's parameters (ϕ being the most important) and a strong fluence-dependent chaotic absorption of photons for realistic pulse envelopes of compact support. The classical dynamics of this rotating anharmonic molecular model driven by an infrared laser satisfy our quantum intuition with respect to ΔJ selection rules and vibrational excitation in the molecule. While quantum mechanically these conditions are built into the calculations, classically the dynamics satisfy these "selection rules" by frequency and phase considerations which are harder to understand intuitively.

The global implication of these calculations for MPE is that the strong (onsets with the turn-on of the electric field) fluence-dependent absorption is due to chaos originating in the interaction of the laser with the rotating molecule's anharmonic pump mode and the intramolecular transfer of energy to the remainder of the molecule. This fluence-dependent absorption had previously been attributed simply to a large density of states in the molecular quasicontinuum, justifying a rate-equation description of the MPE process. *It is interesting that our Hamiltonian system does not require ad hoc homogeneous broadening mechanisms in order to obtain incoherent rate dynamics.*

If a collection of these generic model molecules were placed in a cell and an infrared laser pulse propagated through that cell, then the observable absorption of photons would be described by Beer's law. As many of us already know, this type of absorption was a hallmark of the majority of MPE experiments performed over the last decade. While this is certainly not definitive proof that chaos plays a fundamental role in MPE, it is a completely consistent interpretation of the experimental results.[17]

ACKNOWLEDGMENTS

We would like to acknowledge our earlier collaboration with Harold Galbraith, woodworker and physicist *extraordinaire,* and discussions with Dr. Chris Patterson and Dr. Bob Wyatt.

[1]N. R. Isenor and M. C. Richardson, App. Phys. Lett. **18**, 224 (1971); Opt. Commun. **3**, 360 (1971).

[2]H. W. Galbraith and J. R. Ackerhalt, in *Lasers-Induced Chemical Processes,* edited by J. Steinfeld (Plenum, New York, 1981), pp. 1–44.

[3]J. R. Ackerhalt, H. W. Galbraith, and J. C. Goldstein, Opt. Lett. **6**, 377 (1981); J. R. Ackerhalt and H. W. Galbraith, SPIE **288**, 223 (1981); J. R. Ackerhalt, D. O. Ham, A. V. Nowak, C. R. Phipps, Jr., and S. J. Thomas, IEEE J. Quantum Electron **QE-19**, 1120 (1983).

[4]J.-C. Diels and S. Besnainou, J. Chem. Phys. **85**, 6347 (1986).

[5]E. Mazur (unpublished).

[6]O. P. Judd, J. Chem. Phys. **71**, 4515 (1979).

[7]J. R. Ackerhalt, H. W. Galbraith, and P. W. Milonni, Phys. Rev. Lett. **51**, 1259 (1983); J. R. Ackerhalt and P. W. Milonni, Phys. Rev. A **34**, 1211 (1986).

[8]M. Bixon and J. Jortner, J. Chem. Phys. **48**, 715 (1968).

[9]D. Heller, private communication on the stability of the model used in Ref. 8.

[10]See, for instance, M. J. Lighthill, *Introduction to Fourier Analysis and Generalized Functions* (Cambridge University Press, Cambridge, 1970), p. 67.

[11]G. Casati, B. V. Chirikov, F. M. Izrailev, and J. Ford, in *Stochastic Behavior in Classical and Quantum Hamiltonian Systems,* Vol. 93 of *Lecture Notes in Physics,* edited by G. Casati and J. Ford (Springer, Berlin, 1979).

[12]J. G. Leopold and I. C. Percival, Phys. Rev. Lett. **41**, 944 (1978).

[13]K. A. H. van Leeuwen, G. V. Oppen, S. Renwick, J. B. Bowlin, P. M. Koch, R. V. Jensen, O. Rath, D. Richards, and J. G. Leopold, Phys. Rev. Lett. **55**, 2231 (1985).

[14]J. R. Ackerhalt and P. W. Milonni (unpublished).

[15]H. W. Galbraith, J. R. Ackerhalt, and P. W. Milonni, J. Chem. Phys. **79**, 5345 (1983); in, *Coherence and Quantum Optics V,* edited by L. Mandel and E. Wolf (Plenum, New York, 1984), p. 721.

[16]D. A. Jones and I. C. Percival, J. Phys. B **16**, 2981 (1983).

[17]This work has been presented in a shortened form at the NATO Advanced Research Workshop on Atomic and Molecular Processes With Short Intense Laser Pulses, Lennoxville, Quebec, Canada, 1987.